Available online at www.sciencedirect.com
ScienceDirect
Journal of the European Ceramic Society 30 (2010) 2467–2473
www.elsevier.com/locate/jeurceramsoc

Effect of pH localization on microstructure evolution of deposits during aqueous electrophoretic deposition (EPD)

Mrinalini Mishra [a,c], Sarama Bhattacharjee [a,*], Laxmidhar Besra [a], H.S. Sharma [b], Tetsuo Uchikoshi [c], Yoshio Sakka [c]

[a] *Colloids & Materials Chemistry Department, Institute of Minerals & Materials Technology (IMMT), Bhubaneswar 751 013, India*
[b] *Fuel Chemistry Department, Bhabha Atomic Research Center (BARC), Mumbai, India*
[c] *Nano Ceramics Center, Fine Particle Processing Group, National Institute for Materials Science (NIMS), 1-2-1 Sengen, Tsukuba, Ibaraki 305-0047, Japan*

Received 2 February 2010; received in revised form 17 April 2010; accepted 23 April 2010
Available online 26 May 2010

Abstract

We studied pH localization phenomenon at electrodes under the influence of constant DC voltage during water electrolysis with a view to understand the mechanism of particles consolidation and ordering during aqueous electrophoretic deposition. The pH localization phenomenon was found to depend on applied voltage and initial pH. A pronounced pH localization occurred at higher voltages but the localization was negligible at lower voltages, possibly due to the insufficient water electrolysis. The phenomenon was insignificant when the starting bulk pH was highly acidic or alkaline, but was significant at intermediate pH ranges. During aqueous electrophoretic deposition of monodisperse polystyrene latex spheres, deposition pattern followed a cyclic sequence of aggregation and dispersion of particles at the initial period of time. But after extended period of time, formation of agglomerated particles, multilayers and large clusters was observed. This effect was explained in the light of pH localization.

Keywords: Suspensions; Films; Diffusion; Electrophoretic deposition

1. Introduction

Electrophoretic deposition (EPD) technique has evolved as a widely used ceramic forming process and is increasingly gaining applications in fabrication of thin/thick films, laminates, functionally graded materials, advanced functional coatings, etc., because of its simplicity, low cost and versatility.[1–3] Still, a complete understanding of the mechanism of deposit formation on the electrode is lacking. It is now well recognized that EPD is a three step process: (i) a formation of a stabilized suspension of particles, (ii) the migration of particles towards the deposition electrode under the influence of an electric field, (iii) and the destabilization of the suspension forming deposits on the electrode surface. The mechanism of particle stabilization and electrophoretic migration is understood. However, a clear understanding pertaining to the particle destabilization near the electrode and deposit formation is yet to be achieved. Several mechanisms[4–8] have been proposed by different researchers to explain the experimental results, and by far the most accepted mechanism of EPD was given by Sarkar and Nicholson.[5] They suggested a distortion and thinning of the electrical double layer envelope around the particles by prevailing fluid dynamics due to the applied electric field during electrophoresis. The shear force acting on the double layer envelop streamlines it, making it thinner ahead and wider behind the particles. Sarkar and Nicholson[5] speculated that the cations (co-ions) in the suspension which also move along with the positively charged particles towards the cathode, are in excess and react chemically with the counter ions of the extended double layer tail, thus reducing its thickness and facilitating particle coagulation. However they did not support their speculations with any experimental data. Further, De and Nicholson[9] noted that as the cations carry the major part of the current to the cathode, their concentration in the vicinity of the cathode must decrease because of discharge. Hence, co-ions concentration should be a function of position and time in the EPD cell. They developed a model and showed by theoretical calculations that the H^+ ions concentration gets depleted near the cathode by discharge at the electrode. This results in

* Corresponding author.
E-mail address: saberip@yahoo.com (S. Bhattacharjee).

0955-2219/$ – see front matter © 2010 Elsevier Ltd. All rights reserved.
doi:10.1016/j.jeurceramsoc.2010.04.034

modification of the local pH in the vicinity of the electrode. To maintain the charge transfer process at a virtual equilibrium, the H^+ ions must be supplied by the bulk solution ($x = \infty$) to the cathode ($x = 0$).

The charge transfer process can be described as the following:

$$H^+_{x=\infty} \xrightarrow{\text{transport-process}} H^+_{x=0} + e^- \xrightarrow{\text{charge-transfer}} 1/2H_2 \quad (1)$$

This process will be controlled by the rate of diffusion of H^+ ions from the bulk to the interface. Their calculation predicted the position and time dependent co-ions concentration in the EPD cell. Besra et al.[10] experimentally verified the pH localization theory of De and Nicholson[9] for a 5 vol% alumina suspension through the application of continuous as well as pulsed DC during EPD. They showed the evidence of sharp pH increase in the vicinity of the cathode and concurrent decrease in pH near the anode. However, their study was confined to a single bulk initial pH value of 4.5. It will be of interest to study the extent of pH localization effect as a function of initial pH. Hence, in this paper, we investigated pH localization phenomenon as a function of the initial pH. Further, EPD of spherical mono disperse polystyrene latex (PS) spheres, in aqueous suspension has been investigated under the influence of a continuous DC voltage. The evolution of deposition patterns of PS spheres on the electrode, as a function of time and initial pH was explained on the basis of pH localization effect.

2. Experimental

Water electrolysis experiments were conducted in an EPD cell using silicon wafer as the anode and palladium as the counter electrode, using deionised water (Milli-Q system, Millipore, 0.054 μS/cm). Experiments were conducted at 1 V and 20 V DC, using a source meter (model 2410, Keithley Instruments, Inc., USA). A very low current of about 1 μA, and 1 mA was registered for 1 V and 20 V, respectively due to low conductivity of water. Accordingly, the conductivity of the water was adjusted to about 100 μS/cm by using 7×10^{-4} M KCl solution. The current increased to 20 μA and 20 mA for 1 V and 20 V applied DC, respectively after addition of KCl. To study the pH localization effect, about 30 μl water sample was carefully drawn with a micro-pipette having a sharp tip from near the wall of the electrodes at different intervals of time ranging from 5 s to 15 min during electrolysis. It was then carefully dropped onto an ion sensitive field effect transistor (IS-FET) pH meter (Model no: S2K712) (Fig. 1). The electrodes are compactly placed at the tip of the pH meter. The 30 μl water sample was sufficient to give a reproducible measure of pH. The results reported in the paper are an average of at least five measurements for each point. The measurements were made at varying initial pH ranging from 2.4 to 11, adjusted using 1 M HCl and 1 M NaOH solutions. All the conductivity measurements were made by a conductivity meter (Con510, Eutech Instruments).

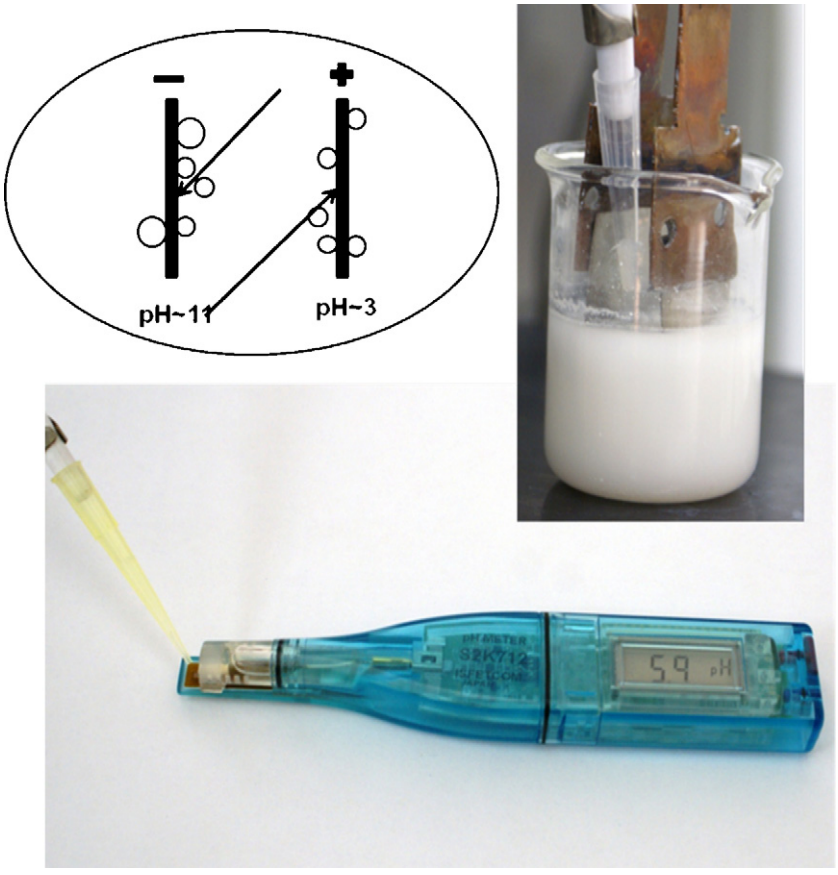

Fig. 1. pH meter used for measurement.

Table 1
Observed pH values near the electrodes with time during water electrolysis as the function of initial pH initial conductivity = 100 μS/cm.

Time (s)	Local pH at the electrodes							
	Initial pH 2.4[a]		Initial pH 4.2[b]		Initial pH 6.6[c]		Initial pH 11.0[d]	
	pH at anode	pH at cathode	pH at anode	pH at cathode	pH at anode	pH at cathode	pH at anode	pH at cathode
5	2.4	2.4	3.6	5.1	4.1	9.6	10.7	10.7
10	2.4	2.4	3.6	7.7	3.8	10.3	10.7	11.0
15	2.4	2.6	3.6	7.7	3.6	10.7	10.7	11.0
30	2.4	2.6	3.7	7.4	3.4	10.6	10.7	11.1
60	2.3	2.4	3.3	8.0	3.2	10.9	10.7	11.0
300	2.3	2.3	3.3	8.4	3.2	11.3	10.3	11.0
600	2.4	2.6	4.1	4.2	3.3	11.4	10.7	11.0
900	2.4	2.6	4.2	4.2	3.3	11.3	10.7	10.4

[a] Conductivity after pH adjustment: 1500 μS/cm; max. current registered: 100 mA.
[b] Conductivity after pH adjustment: 200 μS/cm; max. current registered: 30 mA.
[c] Conductivity: 100 μS/cm (no pH adjustments); max. current registered: 20 mA.
[d] Conductivity after pH adjustment: 800 μS/cm; max. current registered: 100 mA.

To study the deposit formation during aqueous EPD, sulfated polystyrene (PS) latex spheres (400 nm, Aldrich, USA) were chosen as the model system. The variation of their surface charge in water as a function of pH was measured by Streaming potential method[11] using a particle charge detector (PCD 04, Mutek, Germany). EPD was conducted using 0.1 wt% aqueous suspension of PS spheres with conductivity adjusted to about 100 μS/cm by using 7×10^{-4} M KCl solution. The pH of the suspension was 6.6. At this pH, PS spheres acquire a negative charge, and therefore an anodic deposition was expected. EPD was conducted at different time intervals ranging from 5 s to 15 min on a silicon wafer anode with palladium as the counter electrode. The deposit area on the Si wafer was maintained at 1 cm^2, and the inter-electrode distance was fixed at 1 cm. The deposits on anode were dried in a high humid condition for 48 h. The deposit patterns formed were analyzed using SEM.

3. Results and discussion

Electrolysis of pure water at standard temperature and pressure is thermodynamically not favorable. From the Nernst equation, the standard potential for water electrolysis at 25 °C and pH 7 is −1.23 V. The negative sign of the voltage indicates the Gibbs free energy for water electrolysis is greater than zero. However, to make the water electrically conducting, a water soluble electrolyte (i.e. 7×10^{-4} M KCl solution) is added. During the electrolysis, the reduction occurs at cathode [$2H^+$ (aq) + $2e^- \rightarrow H_2$ (g)], while the oxidation reaction occurs at the anode [$2H_2O$ (l) $\rightarrow O_2$ (g) + $4H^+$ (aq) + $4e^-$]. As a result of these reactions, there is an accumulation of H^+ cations near the anode, and a deficit of H^+ near the cathode. Although the electrolyte ions (K^+ and Cl^-) will neutralize some of them, a non-uniform distribution of H^+ is expected due to its high mobility. Fig. 2 shows the variation in pH with time near the anode and the cathode on application of 1 V and 20 V DC during water electrolysis (initial bulk pH 6.6). For the 20 V applied potential, a significant drop in anode pH occurred and pH reduced to about 4.0 within 5 s and dropped further to 3.2 within 1 min. The anode pH eventually stabilized around 3.0 after an extended period of time (900 s). The values presented here are an average of 5 experiments. The drop in anode pH was not very significant for an applied potential of 1 V because of insignificant electrolysis in comparison to 20 V. Similarly, a significant increase in cathode pH was noticed on application of 20 V. The cathode pH increased to 9.3 within 5 s, and reached a pH value of 10.6 after 1 min. The change in cathode pH on application of 1 V was insignificant. At the initial pH of 6.6, the water had a conductivity of about 100 μS/cm. The cell registered a current of 20 μA and 20 mA on application of 1 V and 20 V, respectively. Since pH localization effect was not pronounced at lower voltages, all the subsequent experiments were carried out at 20 V DC.

Table 1 lists the pH values observed near the electrodes when the initial pH was varied from 2.4 to 11.0. It can be seen from the table that at extreme pH values of 2.4 and 11.0, no pH localization effect could be observed. It should be noted that after pH adjustment, the conductivity of water increased to 1500 μS/cm at pH 2.4 and to 800 μS/cm at pH 11.0. At these pH values, a high current (100 mA) flow was registered. The instantaneous

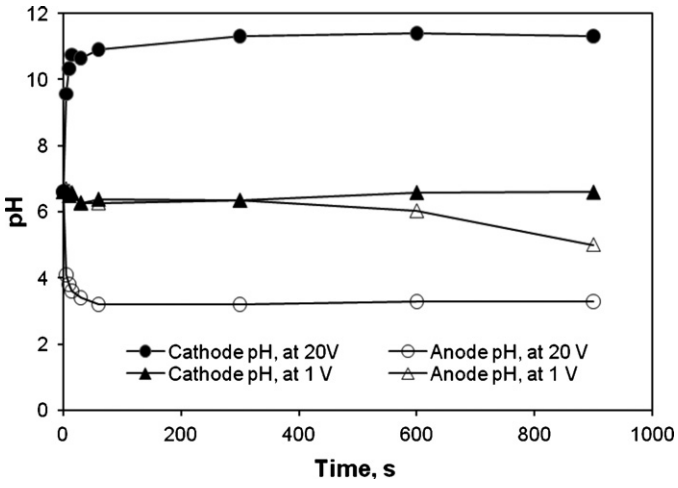

Fig. 2. Variation of local pH at anode on application of 1 V and 20 V DC during water electrolysis.

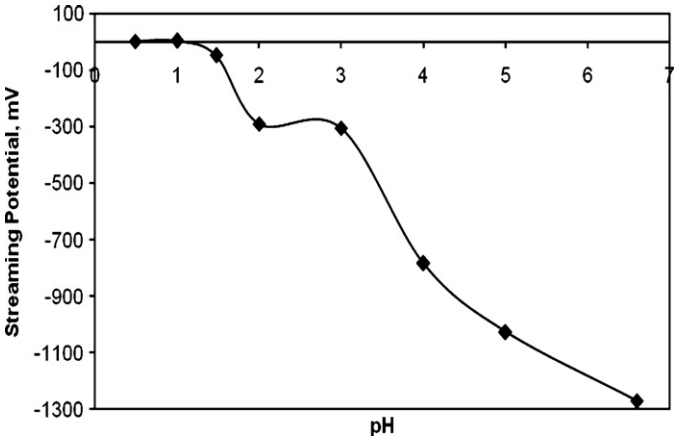

Fig. 3. Variation of streaming potential with pH for 0.01 wt% of PS aq. suspension.

pH localization, if occurring at these extreme pH, were not detectable in the time scale of our measurement. The flux of ion under the existing dynamic state was very high resulting in very fast attainment of equilibrium. However, in the intermediate pH values of 4.2 and 6.6, the pH localization effect was clearly detected. The conductivity of water was 200 μS/cm and 100 μS/cm at pH 4.2 and 6.6, respectively. The registered current flow at these pH values was 30 mA and 20 mA, respectively. Comparatively, the pH localization effect was more pronounced at the neutral pH of 6.6 compared to more acidic pH of 4.2.

The effect of the pH localization on the deposition pattern was investigated during the electrophoretic deposition of polystyrene spheres (400 nm size) in aqueous medium. Fig. 3 shows the variation of surface charge of PS spheres in terms of streaming potential as a function of pH. At the neutral pH range, PS spheres were highly negatively charged; the magnitude of the negative charge decreased progressively with decrease in pH towards acidic values. The point of zero charge of sulfated PS spheres appeared to lie very close to pH 1.0. Fig. 4 shows the variation of pH at close proximity of the anode during EPD of PS

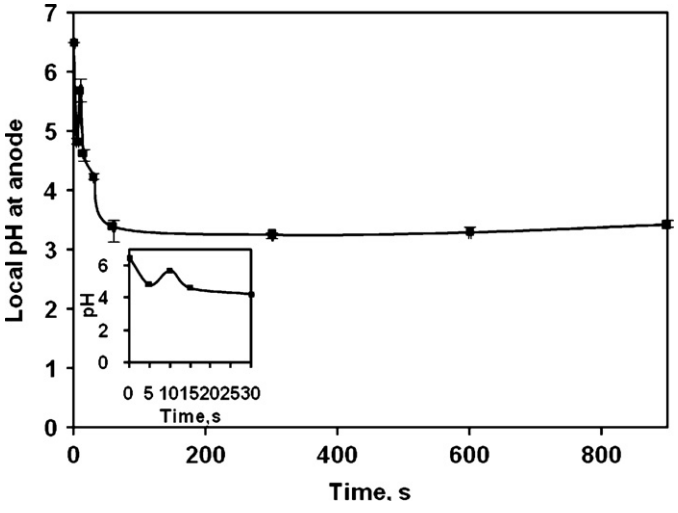

Fig. 4. Variation of local pH at anode on application of 20 V DC during EPD of PS.

spheres (initial bulk pH 6.6). Unlike Fig. 1, some fluctuation in pH was noticed during the initial period of time. Within 5 s, the pH dropped from a value of 6.6 to 4.8, and then reduced further to 4.6 in 10 s; however it again increased to 5.7 in 15 s, then slowly decreased to 3.6 within 1 min and stabilized near that value till the end of the experiment, conducted for 15 min. As soon as the EPD experiment began, an accumulation of H^+ cations occurred near the anode. As a result, initially there was a sharp decrease of pH; however as more bulkier and highly negatively charged PS spheres accumulated near the anode, they neutralized some of the H^+ cations, resulting in an increase in pH. The final pH gradient observed in the EPD cell was determined by the diffusion of the more mobile H^+ cations.

Scanning electron micrographs of deposits depicted through Fig. 5 illustrates the evolution pattern of the deposits with time. It shows that for an applied voltage of 20 V, the deposits followed a cyclic increase and decrease of particle number density in the initial period of time. For example, the number density of PS spheres at 5 s was comparatively lower, but increased at 10 s (Fig. 5a and b). However, the deposit withdrawn at 15 s revealed a reduced number density of PS spheres (Fig. 5c), showing singlets, doublet and triplet clusters. The number density increased again for 30 s (Fig. 5d) and decreased for 1 min (Fig. 5e). When EPD was carried out for an extended period of time, the number density of PS spheres increased slowly from 5 min to 10 min deposits (Fig. 5f and g) and showed a large cluster of PS spheres (Fig. 5h) after 15 min. After 15 min, pH near deposition electrode stabilized at a value which is near the isoelectric point (i.e.p.) of polysterene spheres resulting in decrease in double layer thickness and a consequent decrease in electrostatic repulsion between the depositing spheres promoting coagulation.

During EPD, negatively charged PS spheres moved towards anode along with the co-ions (OH^-). As they come close to the electrode, double layer thickness reduced due to the lowering of pH in the vicinity of the electrode as a result of the pH localization effect. Such a lowering of pH results in coagulation of PS spheres. However, PS spheres do not necessarily form deposit immediately on the electrode. A sensitive balance of forces acting on the PS, namely, the electrophoretic force, the gravity force, the van-der Waals attraction, the electrostatic attraction/repulsion, the steric force, the depletion force, and the hydrodynamic drag will determine its equilibrium separation from the electrode. Depending on the magnitude of the forces, the PS might reside at a considerable distance from the electrode. In the simplest approach, by neglecting the gravity, steric and depletion forces (bare particle), one can model the rest of the forces as (i) an electrode-colloidal interaction force (F_C) i.e. the total interaction force between the electrode and the particle, and (ii) the electrophoretic force (F_E), acting on the particle.[12] F_C is determined by the particle electrode potential and can be represented by double layer repulsion φ_{DL} and van-der Waal interaction φ_{VWD}.

$$F_C = -\frac{d}{dh}(\varphi_{DL} + \varphi_{VWD})$$

where h is the separation of the particle from the electrode.

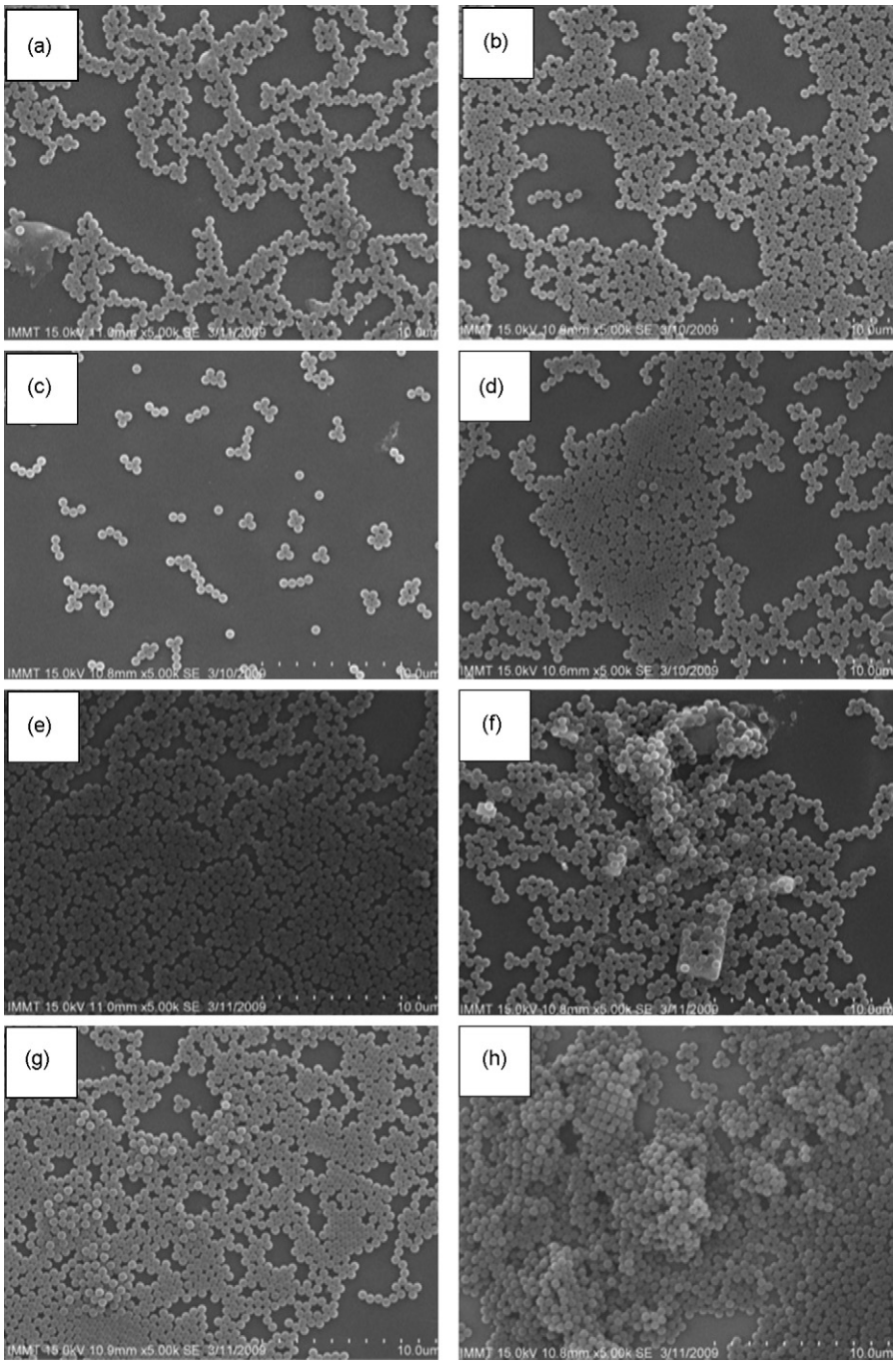

Fig. 5. SEM micrographs of the deposits taken at different interval of time.

In absence of electrical field, the nature of interaction follows DLVO model and is schematically presented by the dotted line in Fig. 6 in arbitrary unit. However, when electric field is present, electromotive force will act on the particle and can be represented by the following equation:

$$F_{\mathrm{E}} = \frac{\mu_{\mathrm{E}}}{\omega_{\mathrm{n}}} E_{\infty}$$

where μ_{E} is the electrophoretic mobility, ω_{n} is the hydrodynamic mobility and E_{∞} is the electric field.

It was shown after detailed analysis by Ristenpart[12] that the combined effect of electrophoretic mobility and hydrodynamic mobility marginally increase the electophoretic force on the particle as it nears the electrode (dotted line in Fig. 6, negative values signifies the attractive nature of the force).

The total force (F_{T}) acting on the particle then can be represented as:

$$F_{\mathrm{T}} = F_{\mathrm{C}} + F_{\mathrm{E}}$$

At large separation distance from the electrode, the electrophoretic force (F_{E}) is the dominant force compared to the electrode-colloidal force (F_{C}). However in close proximity of the electrode, the colloidal force (F_{C}) is higher than the elec-

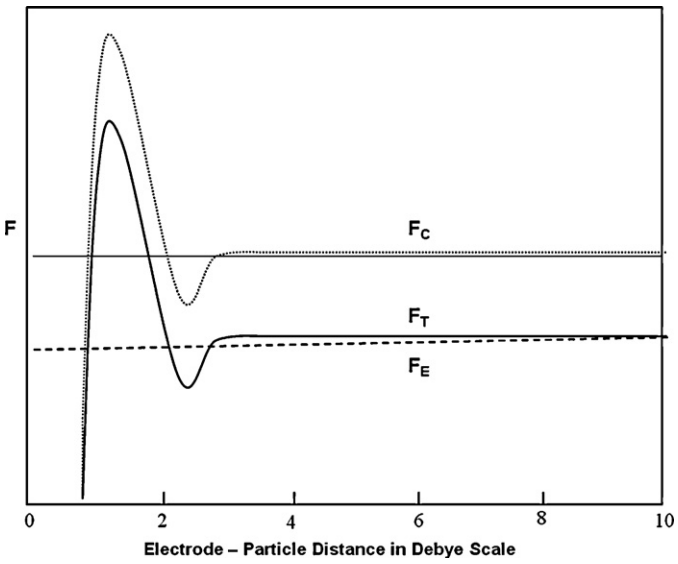

Fig. 6. Schematic presentation of electrode–particle interaction potential during EPD.

trophoretic force (F_E) resulting a barrier. The PS particle will reside in the secondary minimum of the total interaction potential, thereby preventing it to come in close contact with the electrode. In such cases, a significant liquid layer exists between the particle and the electrode, and, consequently, the particles are relatively free to move parallel to the electrode. In the initial period of deposition, the pH decreased very fast and modified the double layer thickness and thereby the local interactions leading to some deposit formation at the electrode. In addition, an electroosmotic slip flow[13] along the surface of the particle which arises due to the presence of the electrode prevented the particle from moving freely, and induced lateral aggregation of the particles on the electrode surface. Chain like aggregates (Fig. 5a) of PS spheres were observed at the initial period, which grew with time (Fig. 5b). But as pH increased, the electrostatic repulsion increased, and the particles may reside in the secondary minimum of potential well, and thereby, capable of lateral movement as reasoned earlier. Hence in such cases, stripping of the deposited particles from the electrode is possible. It may be the cause of the cyclic dispersion and clustering of PS particles observed in the initial period of deposition (Fig. 5c–e). As the deposition time increased, the pH near the anode stabilized near 3 (Fig. 3), resulting in a reduction of the electrostatic repulsion between the spheres and increasing the effective attraction towards anode. This promotes clustering with multilayer formation of the PS spheres (Fig. 5f–h). One point to note here, when the time of deposition increased (more than 1 min), there was an accumulation of O_2 bubbles, that further disturb the deposition of PS spheres. As a result, bare substrate surface was still visible even after 15 min of deposition. Such uneven deposition will modify the local electric field in such a way that freshly incoming particles will tend to deposit preferentially on uncovered areas on the substrate. If EPD will continue for long enough time, the particles will cover the whole area and eventually the deposition yield will decrease due to increased electrical resistance of already deposited particles.

4. Conclusion

The pH localization phenomenon was studied as a function of the initial pH during water electrolysis under the influence of a constant DC voltage. During water electrolysis at extreme pH (2.4 and 11) values, no pH localization effect was detected. In both the cases the pH remained almost unchanged (starting from 5 s) throughout the experiment. However, for the intermediate ranges of starting pH (i.e. for pH 4.2 and 6.6), significant pH localization effect was observed. Comparatively, more pronounced pH localization was observed at more acidic pH of 4.2 than the near neutral pH of 6.6. This may be due to the higher concentration of H^+ at more acidic pH, and higher mobility of H^+ compared to more bulky OH^- group.

The effect of pH localization on deposit formation in an EPD cell was studied using a model system, namely, mono disperse polystyrene sphere of 400 nm diameter at starting pH of 6.6. Deposits withdrawn in the initial period of time exhibited repeated clustering and rarefaction of cluster formation by PS spheres. Unlike the case of water electrolysis, a fluctuation in pH values is apparent in the initial stage. This cyclic change has been attributed to the increase of H^+ ion concentration near the anode and a subsequent neutralization of these ions by the highly negative PS spheres which cause the ephemeral rise in pH value. It was presumed that the initial fluctuation of pH near deposition electrode caused modification of the electrical double layer thickness leading to change in local interactions that affect the balance of the electrode-colloidal forces and electrophoretic forces. After an extended period of time, pH at the vicinity of depositing electrode, determined by the concentration of H^+ ions, tend to approach towards $pH_{i.e.p.}$ of PS spheres. It promoted formation of agglomerated particles and big clusters with multilayer formation. The clustering and agglomerates formation was also non-uniform with some portions of the substrate still uncovered owing to the disturbance created by oxygen bubbles.

Acknowledgments

One of the authors MM is thankful to the Board of Research for Nuclear Science (BRNS) for the Junior Research fellowship. The authors also thank Director, IMMT Bhubaneswar for permission to publish this paper. This study was supported in part by the Grant-in Aid from Board of Research for Nuclear Science (BRNS) India, & World Premier International Research Center Initiative (WPI) on Materials Nanoarchitechtronics, MEXT, Japan.

References

1. Corni I, Ryan MP, Boccaccini AR. Electrophoretic deposition: from traditional ceramics to nanotechnology. *J Eur Ceram Soc* 2008;**28**:1353–67.
2. Besra L, Liu M. A review on fundamentals and applications of electrophoretic deposition. *Prog Mater Sci* 2007;**52**:1–61.
3. Sarkar P, Huang XN, Nicholson PS. Structural ceramic microcomposites by electrophoretic deposition. *J Am Ceram Soc* 1992;**75**(10):2907–9.
4. Tassel VJ, Randall CA. Mechanism of electrophoretic deposition. *Key Eng Mater* 2006;**314**:167–74.

5. Sarkar P, Nicholson PS. Electrophoretic deposition (EPD): mechanism, kinetics and applications. *J Am Ceram Soc* 1996;**79**(8):1987–2002.
6. Fukada Y, Nagarajan N, Mekky W, Bao Y, Kim HS, Nicholson PS. Electrophoretic deposition—mechanisms, myths and materials. *J Mater Sci* 2004;**39**:787–801.
7. Zhitomirsky I. Cathodic electrophoretic deposition of ceramic and organ ceramic materials—fundamental aspects. *Adv Colloids Interface Sci* 2002;**97**:279–317.
8. Hamaker HC, Verwey EJW. The role of ionic depletion in deposition during electrophoretic deposition and other phenomena. *Trans Faraday Soc* 1940;**36**:180–5.
9. De D, Nicholson PS. Role of ionic depletion in deposition during electrophoretic deposition. *J Am Ceram Soc* 1999;**81**(11):3031–6.
10. Besra L, Uchikoshi T, Suzuki TS, Sakka Y. Experimental verification of pH localization mechanism of particle consolidation at the electrode/solution interface and its application to pulsed DC electrophoretic deposition (EPD). *J Eur Ceram Soc* 2010;**30**(5):1187–93.
11. Singh BP, Bhattacharjee S, Besra L. *Ceram Int* 2002;**28**(4):413–7.
12. Ristenpart, W. D., *Electric field induced assembly of colloidal particles*. Ph. D. Dissertation, 2005, Department of Chemical engineering, Princeton University.
13. Solomenstev Y, Bohmer M, Anderson JL. Particle clustering and pattern formation during electrophoretic deposition—a hydrodynamic model. *Langmuir* 1997;**13**:6058–68.